Developmental Biology 331 (2009) 26–37

Contents lists available at ScienceDirect

Developmental Biology

journal homepage: www.elsevier.com/developmentalbiology

Hedgehog signaling patterns mesoderm in the sea urchin

Katherine D. Walton [a], Jacob Warner [a], Philip H. Hertzler [b], David R. McClay [a,*]

[a] Department of Biology, Duke University, Box 90338, Durham, NC 27708, USA
[b] Department of Biology, Central Michigan University, Mount Pleasant, MI 48859, USA

ARTICLE INFO

Article history:
Received for publication 23 May 2008
Revised 30 March 2009
Accepted 17 April 2009
Available online 23 April 2009

Keywords:
Hedgehog
Patched
Smoothened
Morphogenesis
Endoderm
Mesoderm
Signal transduction

ABSTRACT

The Hedgehog (Hh) signaling pathway is essential for patterning many structures in vertebrates including the nervous system, chordamesoderm, limb and endodermal organs. In the sea urchin, a basal deuterostome, Hh signaling is shown to participate in organizing the mesoderm. At gastrulation the Hh ligand is expressed by the endoderm downstream of the Brachyury and FoxA transcription factors in the endomesoderm gene regulatory network. The co-receptors Patched (Ptc) and Smoothened (Smo) are expressed by the neighboring skeletogenic and non-skeletogenic mesoderm. Perturbations of Hh, Ptc and Smo cause embryos to develop with skeletal defects and inappropriate non-skeletogenic mesoderm patterning, although initial specification of mesoderm occurs without detectable abnormalities. Perturbations of the pathway caused late defects in skeletogenesis and in the non-skeletogenic mesoderm, including altered numbers of pigment and blastocoelar cells, randomized left–right asymmetry of coelomic pouches, and disorganized circumesophageal muscle causing an inability to swallow. Together the data support the requirement of Hh signaling in patterning each of the mesoderm subtypes in the sea urchin embryo.

Introduction

The Hedgehog (Hh) signaling pathway was discovered in *Drosophila* and since then has been found to direct developmental processes throughout the animal kingdom including *Nematostella* (Matus et al., 2007), sea urchin (Walton et al., 2006), leech (Kang et al., 2003), amphioxus (Shimeld, 1999), zebrafish (Krauss et al., 1993), *Xenopus* (Roelink et al., 1994), chick (Riddle et al., 1993), mouse (Echelard et al., 1993), and human (Chang et al., 1994). Strikingly, the only animal model system lacking the complete pathway to date is *Caenorhabditis elegans* (Aspock et al., 1999; Kuwabara et al., 2000). The pathway is composed of many components but four molecules central to the pathway are the Hh ligand, its receptor Ptc, co-receptor Smo, and the downstream transcription factor Cubitous interruptus (Ci or Gli in vertebrates, henceforth referred to as Gli). As a simplified sequence of Hh signal transduction, in the absence of the Hh ligand, the Ptc receptor inhibits the activity of Smo thus allowing the Gli transcription factor to be proteolytically cleaved to a shortened form that represses transcription. When Hh binds to Ptc, the inhibition of Ptc on Smo is alleviated. Smo activity then leads to the stabilization of the long form of the Gli transcription factor, which then activates transcription of target genes (details of the pathway, including other transducing components, are reviewed in (Huangfu and Anderson, 2006; Ingham and McMahon, 2001; Lum and Beachy, 2004).

In the sea urchin, through a survey of the *Strongylocentrotus purpuratus* genome, single homologous genes were identified for each of the main Hedgehog pathway components (Walton et al., 2006). Each of the four major genes in the pathway was cloned in *Lytechinus variegatus* and their spatial and temporal expression analyzed. In *L. variegatus* (Lv) Hh is expressed in the endoderm while Ptc and Smo are expressed in the neighboring mesoderm, a theme that is similar to expression of these components in other phyla (Walton et al., 2006; and this study). These expression profiles obviously suggest a role for paracrine Hh signaling from the endoderm to the mesoderm. This paper reports tests of that hypothesis.

In the sea urchin, embryonic mesoderm is subdivided into the skeletal mesoderm produced by the primary mesenchyme cells (PMCs) and the non-skeletal mesoderm (NSM). The founder cells of the skeletal mesoderm arise precociously as micromeres from the unequal fourth cleavage at the vegetal pole of the embryo. These cells ingress into the blastocoel, and as PMCs, form a ring around the archenteron with two concentrations of cells forming at the sites where skeletogenesis initiates. Patterning information for skeletogenesis is delivered from the overlying ectoderm (Armstrong et al., 1993; Armstrong and McClay, 1994; Duloquin et al., 2007; Peterson and McClay, 2003), and from the endoderm (Benink et al., 1997; Croce et al., 2006).

Non-skeletogenic mesenchyme cells (NSM) arise later at around 8th–9th cleavage as a result of a subdivision of endomesoderm into endoderm and NSM. The NSM later differentiates into to four different cell types: pigment cells (Calestani et al., 2003), blastocoelar cells (Hibino et al., 2006b; Rast et al., 2006), coelomic pouches, the left one of which eventually forms the rudiment of the adult embryo (Davidson et al., 1998; Gustafson and Wolpert, 1963), and muscle cells that surround the foregut of the larva and organize peristaltic

* Corresponding author. Fax: +1 919 660 7293.
E-mail address: david.mcclay@duke.edu (D.R. McClay).

0012-1606/$ – see front matter © 2009 Elsevier Inc. All rights reserved.
doi:10.1016/j.ydbio.2009.04.018

contractions equivalent to swallowing (Burke and Alvarez, 1988; Wessel et al., 1990; Beach et al., 1999; Venuti et al., 1993,1991).

Here, we show that in the sea urchin *L. variegatus*, Hh in the endoderm signals to both of the adjacent mesodermal lineages and influences patterning of the structures derived from those tissues. Perturbations of Hh signaling causes skeletal defects reflecting an influence on the PMCs, as well as causing alterations in pigment and blastocoelar cell numbers, randomization of left/right coelomic pouches, and disorganization of muscles, thereby affecting each of the mesodermal cell types. Thus, Hh signaling in the sea urchin, as in other organisms, plays an important role in subdividing and dictating pattern in mesodermal structures.

Materials and methods

Animals and drug inhibitions

L. variegatus adults were obtained from Florida (Sea Life, Tavernier, FL), or from the Duke University Marine Laboratory. The Hh pathway was inhibited with Cyclopamine Biomol, Plymouth Meeting, PA Cat# GR-334. Embryos were added to SW containing Cyclopamine. A range of concentrations were tested and it was determined that 6.25 μM was the most effective dose based on optimal phenotypes seen with other inhibitors of the Hh pathway.

RNA extraction and cloning

RNA was extracted from whole embryos at various stages of development with Trizol reagent (Invitrogen Cat# 15596-026) followed by chloroform extraction, precipitation, ethanol washes and resuspension in nuclease free water. Hh, Ptc, and Smo sequencing primers were designed within highly conserved regions of the predicted genes based on the *S. purpuratus* (Sp) genome sequence. PCR amplification (proofreading polymerase, Advantage2 (ClonTech Cat# 639206)) used a cDNA template that had been reverse transcribed from *L. variegatus* (Lv) RNA. The RNA was extracted from embryos between late gastrula and 3-day pluteus stages. PCR products were cloned intopGEMT Easy vector (Cat# A1360) and sequenced. Using the Lv sequence obtained in this way, nested primers for Rapid Amplification of cDNA Ends (RACE) were designed. 5′ and 3′ RACE cDNA was prepared from RNA extracted from late gastrula and 3-day-old embryos using the Ambion First Choice RLM-RACE kit (Cat#1700). Products were again cloned into pGEMT Easy vector and sequenced with ABI prism Big Dye Termination using M13 forward and M13 reverse primers. Assembly of the various RACE and PCR products was performed in Sequencher 4.5 and new primers were designed to amplify the full-length sequence of the genes by PCR with Advantage 2. These products were cloned into pGEMT Easy vector to use as templates for preparation of RNA whole mount in situ hybridization probes. Full-length sequences for LvHh, LvPtc and LvSmo can be found at: AF059606, DQ916038, and DQ915163 respectively.

Full-length Hh was cloned as described above and cloned into pCS2 vector using primers to add ClaI and XbaI sites during the PCR amplification with Pfu polymerase of the full-length sequence (primers were: 5′-ccatcgatatggttcatgcggacatgg-3′ and 5′-gttctaga-caacctatacatcaaagcctgggtatag-3′). Following restriction enzyme digest, the PCR product was ligated into pCS2 and amplified in XL-1 Blue *E. coli* electrocompetent cells. Purification of the plasmid DNA was performed using the Qiagen miniprep kit and the clone's sequence was confirmed by sequencing. Larger preparations of plasmid DNA then amplified from frozen bacterial stocks and purified by Qiagen midiprep kit. Full-length Hh in pCS2 was linearized with NotI restriction enzyme and used as a template to prepare mRNA for injection using the Ambion Sp6 mMESSAGE mMACHINE High Yield Capped RNA Transcription Kit (cat# 1340). RNA was diluted with Rhodamine dextran in 40% glycerol and injected at a concentration of 0.58 pg/pl.

Mutagenesis to produce Activated Smoothened (ActSmo)

Full-length LvSmo was cloned as described above and cloned into pCS2 vector using primers to add ClaI and XhoI restriction sites during the PCR amplification of the full-length sequence (primers were: 5′-cccatcgatggtgcaatggatggattactgggttcaaag-3′ and 5′-ggactcgagtcatatg-tacattacagcataaaacaaggcctgaaattgaaagttgcc-3′). Following restriction enzyme digestion, the PCR product was ligated to pCS2 and amplified in XL-1 Blue *E. coli* electrocompetent cells. Purification of the plasmid DNA was performed using the Qiagen miniprep kit. Sequencing of the plasmid confirmed the sequence, which was then used as a template for in vitro mutagenesis to prepare the Activated Smo (ActSmo) clone. ActSmo is the result of a single base-pair mutation of G to T resulting in an amino acid change of W to L consistent with the mouse Smo activating mutation of W539L (SmoA1) described in Taipale et al. (2000). Mutagenesis was performed by PCR amplification with Pfu using overlapping primers bearing the base-pair change to amplify the entire plasmid. The primers used for mutagenesis were: 5′-gcatcg-ccatgagtatgttggtctggacccccgcaac-3′ and 5′-gttgcgggggtccagaccaaca-tactcatggcgatgc-3′. Following mutagenesis the PCR products were digested with DpnI to remove the wild type Smo methylated template DNA used in the PCR reaction. The remaining PCR-generated activated Smo plasmid containing the single base-pair change was then electroporated into XL-1 Blue *E. coli* for amplification, purification and sequencing. Sequencing confirmed the single base-pair mutation resulting in activated Smo (ActSmo). mRNA was prepared from ActSmo in the pCS2 vector by linearization with NotI and transcribed using the Ambion Sp6 mMESSAGE mMACHINE High Yield Capped RNA Transcription Kit (cat# 1340).

Injection of morpholinos and RNA

Morpholino antisense oligonucleotides (MASOs) were designed to bind near the start sites of the mRNA sequence to block translation. Two non-overlapping MASOs were designed and tested for Ptc: 5′-caggtactgcccaacgctccatatc-3′ and 5′-gatacataggtttcctgccacagtc-3′. The Hh MASOs were 5′-ctttaccatgtccgcatgaaccatg-3′and 5′-ctggtaaaagcat-gaggcgatccat-3′, and LvSmo was 5′-tttgaacccagtaatccatccattg-3′. MASOs were obtained from Gene Tools, Philomath, OR. The MASOs were diluted with Rhodamine dextran in 40% glycerol and injected at concentrations between 0.06 mM and 0.75 mM with delivery of about 1 pl per egg.

A number of controls gave us confidence that the MASOs targeted specific molecules in the Hh pathway. First, MASOs that should inhibit activation of the pathway (Hh MASO, Smo MASO) had the same inhibitory effect, and that effect matched the phenotype of an independent test of Hh pathway inhibition using cyclopamine (and jervine, data not reported). MASOs that should activate the pathway by knocking down Ptc (two non-overlapping MASOs) both gave the same phenotype and two independent activators of the pathway matched those phenotypes: Hh over-expression and expression of activated Smo. Further, control MASOs at higher concentrations in each experiment had no abnormal phenotype, and MASOs to proteins not associated with the Hh pathway gave distinct phenotypes. In each case the phenotypic effect was dose dependent. Full-length Hh and Activated Smo mRNA were prepared as described above and diluted with Rhodamine dextran in 40% glycerol for injection at the 1 cell stage.

In situ analysis

Probes were prepared as described in Walton et al. (2006). The Hh probe was extended to include 5′ and 3′ UTR regions to provide a

longer template for the in situ probe. For this clone, the primers were: 5′-cagggtcgctcaaactgtcg-3′ and 5′-catgaatgccttgtcatagagc-3′. Plasmids were electroporated into XL-1 Blue *E. coli* for amplification and then purified with Qiagen miniprep and midiprep kits. Plasmids were sequenced to verify their identity and orient direction of the clone. Following linearization, 4 μg of plasmid was used as a template for transcription of digoxigenin labeled RNA probes as described in Lepage and Gache (1990). Hh was linearized with NcoI and transcribed with Sp6, Ptc was linearized with SpeI and transcribed with T7, and Smo was linearized with ClaI and transcribed with Sp6. The Delta probe was prepared as in Sweet et al. (2002). The clone sequences of GCM and AA29 in pGEMT Easy vector are available at: bankit1040888 and bankit1040906. The GCM and AA29 clones were linearized with NcoI and NdeI and transcribed with Sp6 and T7 RNA polymerases respectively. Partial clones for SoxE and Scl were amplified by PCR from cDNA using primers designed from the S. *purpuratus* sequences and ligated into pGEMT Easy vector and sequences. Those clones can be found at: Scl bankit1038583, SoxE bankit1040875, SoxE and Scl were linearized with SpeI and digoxigenin labeled probes were transcribed with T7.

Fixation and hybridization

Embryos were fixed in 4% PFA/ASW containing 10 mM EPPS for 1 h at room temperature, rinsed briefly with ASW and stored in methanol at −20 °C. Stored embryos were rehydrated and prehybridized with 50% formamide, 25% 20× SSC pH 5.0, 0.001% of 50 mg/ml heparin, 0.001% of 50 mg/ml yeast tRNA, and 0.002% of 50% Tween20 for 1 h at 65 °C. 1 ng/μl of RNA probes labeled with digoxigenin were hybridized overnight at 65 °C (or 40 °C for pluteus stages of embryos). Following hybridization with the RNA probe, embryos were washed through hybridization solution, 2× SSCT, 1× SSCT and 0.1× SSCT at 65 °C. Washed embryos were then blocked for 1 h at room temperature in 0.5% BSA/2% heat-inactivated goat serum in 1X TBST. Antidigoxigenin antibody was incubated at 1:2000 in blocking solution for 2 h at room temperature. Embryos were then washed 5 times with 1× TBST and color reactions were performed with NBT/BCIP for a few hours at room temperature or overnight at 4 °C.

Antibody staining

Embryos were fixed in ice-cold methanol for several minutes and rinsed with 1× PBST. Following fixation embryos were blocked in PBST plus 4% normal goat serum (NGS) for 1 h at room temperature and then incubated in primary antibody diluted in 4% NGS overnight at 4 °C. Dilutions for antibodies were: 1:750 for myosin (Wessel et al., 1990), 1:50 for 1e11 (Burke et al., 2006) and 1:200 for 1d5 (McClay et al., 1983), 1:200 for NSM-2 (Sweet et al., 1999) and rabbit anti-serotonin antibody (Sigma). After the primary antibody incubation, embryos were washed 4 times with 1× PBST and incubated in secondary antibody diluted at 1:200 in 4% NGS for 1 h at room temperature. A Zeiss 410 or 510 confocal microscope was used to image the antibody staining at 40× magnification. Figures were compiled from stacks of the images with the Zeiss confocal software.

Feeding beads

Twenty embryos were added to 1 ml of ASW. One drop of a stock solution of 100 ml ASW containing 50 μl of 10 μm polystyrene beads (Polysciences, Inc Warrington, PA cat# 17136) was added to the culture and embryos were allowed to feed on the beads for 30 min. After 30 min embryos were imaged and their ability, or lack thereof, to ingest beads was recorded. Movies imaged feeding embryos. 2000 images were captured continuously on a Zeiss Axio Imager widefield fluorescence microscope at 40× and 20× magnification for 5 min for both controls and Ptc MASO-injected embryos. Stacks were made into movies compressed into 1 min and 12 s using Metamorph 7.1 software.

Embryo recombination experiments

Eggs were fertilized in ASW with PABA and injected at the one cell stage with either Ptc MASO (1 pl of 0.75 mM MASO diluted with Rhodamine dextran and FITC in 40% glycerol) or with 1 pl of FITC in 40% glycerol. Embryos were transferred to calcium free seawater and animal and vegetal halves were microsurgically separated between the 32 and 60 cell stages and reciprocally recombined. Following recombination the chimeras were transferred to ASW and cultured for two days before being fed beads and immunostained (as above).

Results

The Hh ligand is transcribed in endoderm while the Ptc and Smo co-receptors are transcribed in the mesoderm

Sea urchin Hh, Ptc and Smo were identified during the annotation of the *S. purpuratus* (Sp) genome (Walton et al., 2006). Northern analysis and quantitative PCR data showed that Hh is expressed

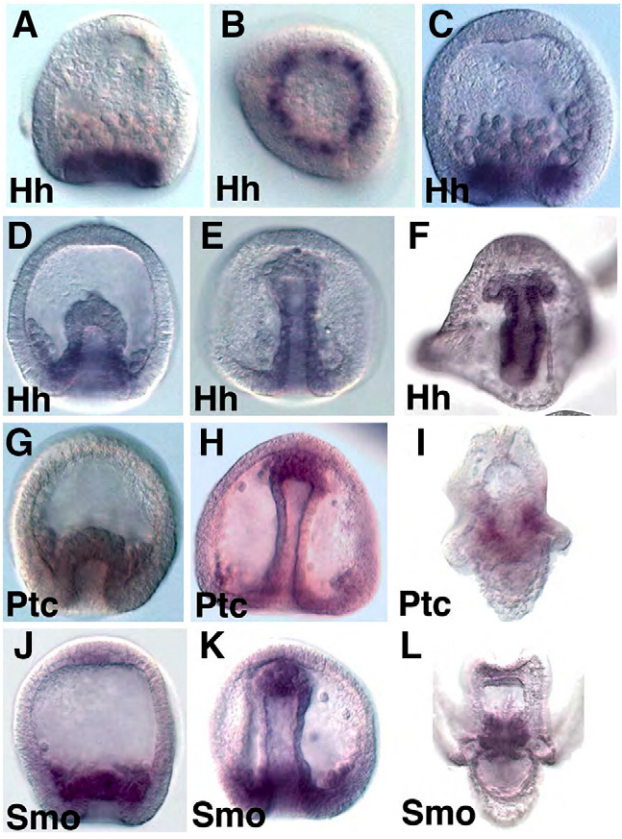

Fig. 1. Whole mount RNA in situ hybridization of Hh (A–F), Ptc (G–I) and Smo (J–L). In (A) and (B, ventral view), Hh expression is first detected at mid to late mesenchyme blastula stages as a single ring of cells in the endoderm. By early gastrula (C) the ring expands to a ring two–three cells wide, and during gastrulation (D, E) Hh expression is detected throughout the gut but not in the NSM at the tip of the archenteron. In pluteus larvae Hh expression spans the entire gut to the boundary of the coelomic pouches seen budding off the side of the foregut in (F). Ptc is first observed localized to the NSM at the beginning of gastrulation (G). At late gastrulation Ptc is still seen in the NSM and a new site in the PMCs surrounding the base of the archenteron (H). At the pluteus stage Ptc is expressed in the two coelomic pouches (I). Smo is first localized to the NSM at the beginning of gastrulation (J). At the end of gastrulation Smo is observed in the NSM at the tip of the archenteron (K), throughout the PMCs surrounding the NSM, and perhaps at a low level in the hindgut, though most of the staining observed in is in out-of-focus PMCs. At the pluteus larva stage Smo is observed in coelomic pouches (L).

zygotically with accumulation beginning just prior to mesenchyme blastula stage and continuing throughout gastrulation (Walton et al., 2006). Preliminary in situ hybridization analyses revealed that Hh is expressed in the endoderm. Quantitative PCR of Ptc and Smo indicated that these co-receptors are expressed prior to gastrulation, but in situ analysis first detects localized Ptc and Smo in the non-skeletogenic mesoderm (NSM) and later in the primary mesenchyme cells (PMCs) (Walton et al., 2006). A more detailed in situ analysis shown in Fig. 1 corroborates and extends those earlier observations. Hh is expressed in the endoderm beginning just prior to invagination of the archenteron as a single torus of cells surrounding the future blastopore (Fig. 1B). Hh expression expands and persists in the gut to the pluteus stage (Fig. 1F), and is not expressed in the non-skeletogenic mesoderm at the tip of the archenteron (Figs. 1C–F). Ptc and Smo are first localized by in situ in the NSM and in PMCs (Figs. 1G, J) at the beginning of gastrulation. At the end of gastrulation Ptc and Smo are observed in the NSM at the tip of the archenteron, in PMCs surrounding the archenteron, and possibly in a region of the hindgut at the boundary between endoderm and ectoderm, though most of that vegetal staining seen in Figs. 1H and K is attributable to PMCs. In the pluteus larva Ptc and Smo become confined to the coelomic pouches and muscle, including circumesophageal muscle (Figs. 1I, L).

Perturbations of the Hedgehog pathway affect patterning of the mesoderm

Perturbations of Hh pathway members addressed the function of the Hh signaling pathway during development. We expected that if one Hh pathway member gave a particular phenotype, similar perturbations of other pathway members should show a very similar phenotype. To test that prediction Hh signaling was increased by three treatments: 1) knockdown of the Hh receptor Ptc with a Ptc MASO (2 different MASOs from non-overlapping regions gave identical phenotypes), thereby allowing Smo to actively signal; 2) expression of a constitutively activated form of Smo (ActSmo); or 3) over-expression of full-length Hh. Similar results were obtained with each treatment as described in detail below. Alternatively, the pathway was inhibited by four treatments: 1) Hh, and 2) Smo were separately knocked down with morpholinos; 3) the pathway was inhibited using the drug cyclopamine; or 4) Ptc was over-expressed. In each case these perturbations affected patterning of PMCs and NSM subtypes. The perturbations that activated the pathway tended to be similar to one another, and the perturbations that knocked down the pathway were similar to one another as well. Manipulation of the Hh pathway had no detectable impact on specification or patterning of ectoderm and little, if any, impact on endoderm development. These results are detailed below.

Perturbations that activated the Hh pathway

Ptc MASO-injected, constitutively activated Smo-expressing, and Hh over-expressing embryos developed normally compared to controls until gastrulation based on phenotype and on QPCR analysis of transcription factors known to participate in germ layer specification (data not shown). This was somewhat surprising given that earlier QPCR measurements indicated that some Hh pathway members were expressed at significant levels early in cleavage. Apparently the lack of Hh prior to gastrulation and perhaps of other pathway members prevents the full pathway from functioning prior to Hh synthesis.

Normally PMCs ingress at 10 h and the embryo arrives at the pluteus larval stage by about 22 h. At 0.75 mM the Ptc MASO-injected embryos were delayed in gastrulation (Fig. 2B). Gastrulation was completed with a delay and a skeleton formed in those embryos, however the skeleton was abnormally patterned in most embryos, and

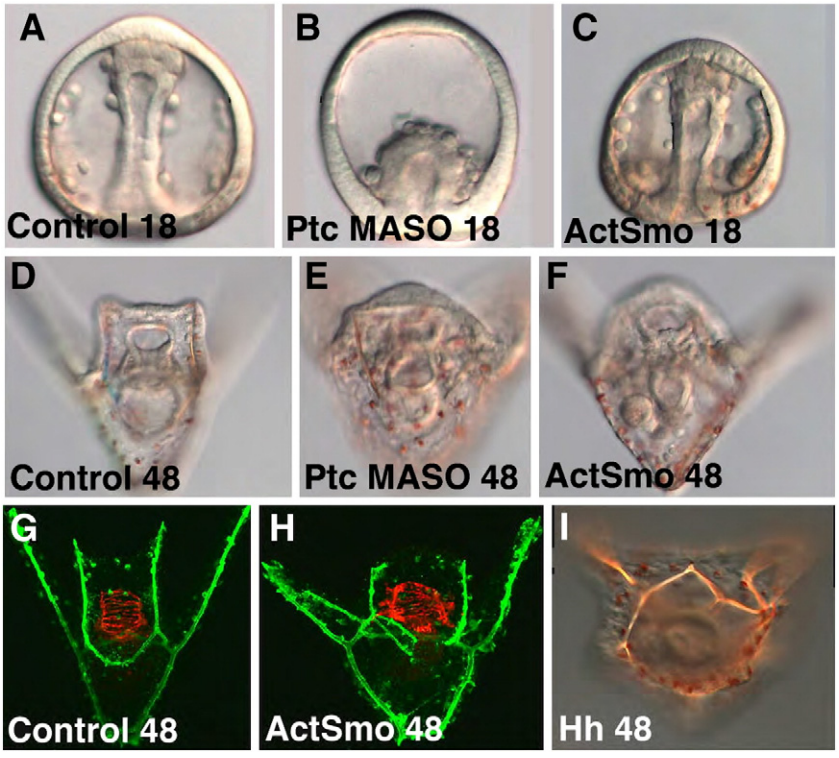

Fig. 2. Activation of the Hh pathway. The Hh pathway was activated by three treatments, injection of a Ptc MASO which blocked Ptc activity thereby allowing Smo to be active (B, E), injection of RNA construct that produced constitutively activated Smo (C, F, H), or over-expression of Hh (I). At 18 h, the Ptc MASO (0.75 mM) delayed gastrulation (B) relative to controls (A), but development caught up and at 48 h the phenotype was mild with an increased number of pigment cells (E), relative to controls (D). Activated Smo did not delay gastrulation at 0.63 pg/pl with ca. 1 pl injected per egg. However, at 48 h there were an excess number of pigment cells (F), an abnormal skeletal pattern and abnormal circumesophageal musculature (H), relative to controls at 48 h (D, G). At 48 h, embryos expressing extra Hh (ca. 1 pl at 0.58 pg/pl) displayed an abnormal skeleton (I).

there were extra pigment cells observed. Since Ptc receptors are not detected in the endoderm the delay could either be due to an effect of Ptc on the NSM's role in initiating invagination (Beane et al., 2006; Croce et al., 2006), or the delay could be a simple consequence of a generalized developmental delay sometimes seen with morpholinos.

Expression of a constitutively activated form of Smo (ActSmo) affected PMC and NSM patterning as well. ActSmo was created by a single base-pair mutation changing G to T resulting in an amino acid change of W519L, similar to human Activated Smo (Taipale et al., 2000; Xie et al., 1998). ActSmo, produced phenotypes similar to the loss of Ptc expression (Figs. 2C, F, H), though, unless higher levels of ActSmo RNA were injected, there was no delay in gastrulation (Fig. 2C). At 0.63 pg/pl ActSmo-expressing embryos had excess pigment cells (Fig. 2F). The ActSmo-injected embryos superficially appeared normal by the pluteus larva stage, however they often displayed an increased number of pigment cells (Figs. 2K, L). Quantification of NSMs with over-expression of ActSmo was determined by immunostaining with the SMC-2 antibody that marks NSM cells in 2-day-old plutei. Using this approach an average increase of 17% NSMs in the blastocoel ($p = 0.0049$) was observed. In a separate count, pigment cells were increased by an average of 21.8% in ActSmo-injected embryos ($p = 0.0001$). Finally, ActSmo caused abnormal skeletal patterning and abnormal circumesophageal muscle patterning (Fig. 2H). Muscle mis-patterning is examined in greater detail below.

Increased Hh signaling caused similar abnormalities. Hh was over-expressed by injection of Hh RNA at 0.58 pg/pl. Fig. 2I shows an example of skeletal mis-patterning and an increased number of pigment cells, again similar to what was seen with the other Hh pathway members when the pathway was over-activated. Unless Hh was vastly over-expressed (greater than 2 pg/pl) the only phenotypes observed were alterations in mesodermally derived structures.

Perturbations that inhibited the Hh pathway

The four separate inhibitions of the Hh pathway resulted in similar phenotypes, in each case complimentary to the results seen with activation of the pathway. First, two different morpholinos were tested to Hh. Figs. 3B and D show embryos that had been injected with of Hh MASO2 at 0.06 mM. Those embryos had a truncated skeleton at 48 h relative to controls (Figs. 3B compared to A), and had mis-patterned circumesophageal musculature (compare the red muscle in Figs. 3B, D with controls in A,C). Treatment with the Hh inhibitor cyclopamine caused a truncated skeleton and a reduced number of pigment cells at 24 h (Fig. 3F), relative to controls at the same stage (Fig. 3E), an observation made with cyclopamine in a previous set of experiments (Egana and Ernst, 2004). The same suite of abnormalities was observed with a morpholino to Smo (Smo MASO, 0.375 mM). Bilateral skeletons formed but the patterning was abnormal (Fig. 3H) and there was a reduced level of pigmentation observed. Development was delayed as well as seen in the 22 h embryo shown in Fig. 3H, but those embryos later caught up to the controls, except for persistence of the mesodermal abnormalities. When the Hh co-receptor Ptc was over-expressed at 0.5 pg/pl, it should have produced an increased inhibition of Smo function. This apparently happened since the resulting phenotypes were similar to other pathway inhibitions that altered skeleton patterning (Figs. 3I, J) and reduced pigmentation (data not shown). Thus, alteration of the Hh pathway caused disruption in patterning of the skeleton, circumesophageal muscle, and altered numbers of pigment cells, in each case mesodermal derivatives.

Hh signaling begins just prior to gastrulation, after early mesodermal specification is completed

Although an earlier study showed by QPCR that some members of the Hh pathway are expressed prior to mesenchyme blastula stage (Walton et al., 2006), expression of Hh itself doesn't begin until mesenchyme blastula stage (Fig. 1), and none of the perturbations, either positive or negative, suggested earlier disruptions in specification, unless the disruptor was injected at very high levels, levels that were likely to include non-specific or toxic effects. By QPCR we examined a number of transcription factors known in early specification events and found that none were affected by the perturbations, positive or negative, as described above. Thus it was

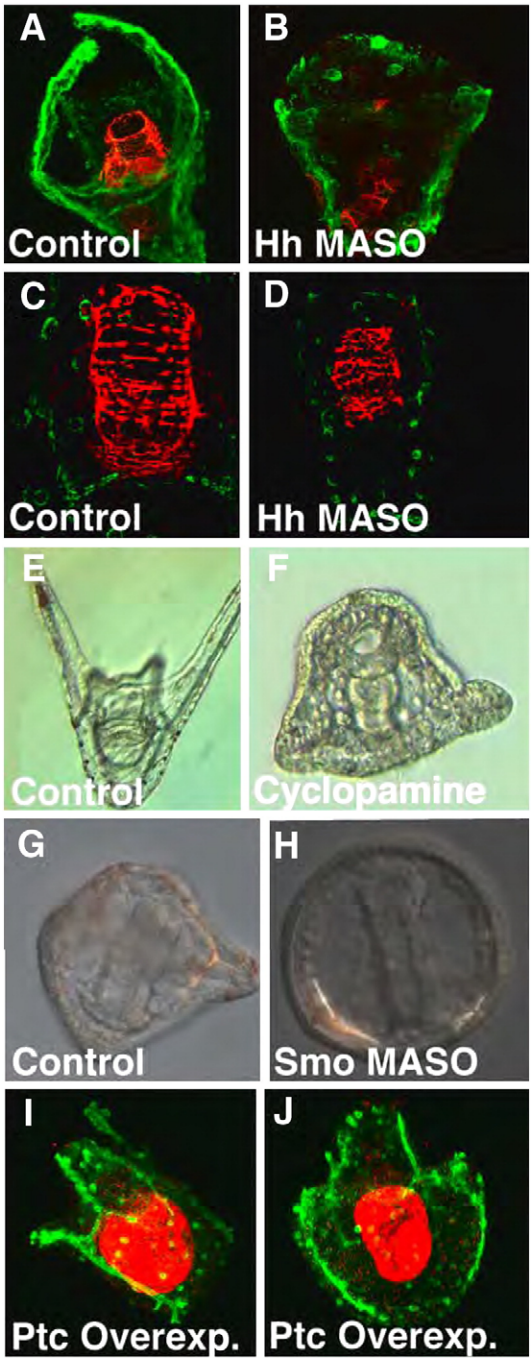

Fig. 3. Inhibition of the Hh pathway. The Hedgehog pathway was blocked by four different treatments. In (B and D) an Hh MASO (60 μM) caused skeletal (B) and circumesophageal muscle abnormalities (B, D) relative to controls (A, C). Treatment with Cyclopamine (6.25 μM) truncated skeletal development and reduced the number of pigment cells (F) relative to controls at 48 h (E). A Smo MASO (375 μM) caused a truncated skeleton and reduced pigmentation (H) relative to controls at 22 h (G). Over-expression of Ptc (0.5 pg/pl) caused an abnormal skeleton to develop (I, J). In (A–D and I, J), the skeleton is stained with an antibody to MSP130 (green). In (A–D) circumesophageal muscle is stained with anti-myosin (red). In (I, J) the midgut and hindgut is stained with an endoderm marker (red).

not likely that Hh signal transduction had a quantitative impact on early PMC or NSM specification sequences. Though QPCR studies failed to indicate a quantitative impact on early specification of perturbed embryos, it was possible that the Hh pathway perturbations had a spatial impact on specification. For this reason we examined several known NSM markers that are present at mesenchyme blastula stage, first to ask whether the perturbations had significant impacts on early expression or position of expression of gene regulatory network (GRN) members.

Hh signaling was perturbed by loss of Ptc (Ptc MASO), which activates the pathway wherever Smo is expressed, by expression of activated Smo (ActSmo mRNA), or by inhibition of Hh expression, and the expression of NSM markers was assessed by whole mount in situ hybridization (Figs. 4 and 5). AA29 is a marker for all NSM cells (Croce

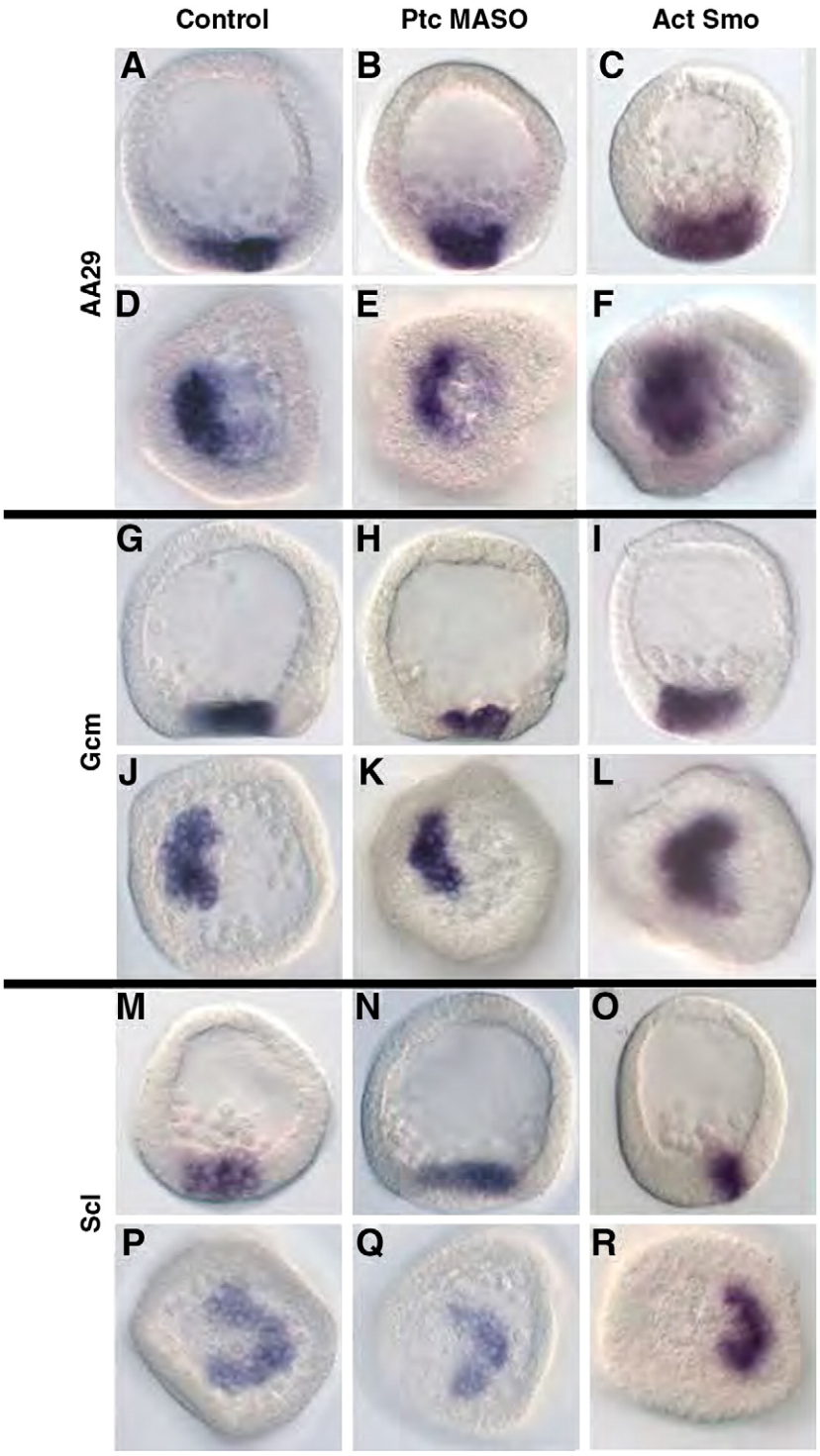

Fig. 4. In situ analysis of non-skeletogenic mesoderm markers at the mesenchyme blastula stage. For each in situ imaged both a lateral view (A–C, G–I, M–O), and a vegetal view (D–F, J–L, P–R) are shown. (A, D, G, J, M, P) control embryos; (B, E, H, K, N, Q) embryos injected with Ptc MASO (0.75 mM); (C, F, I, L, O, R) embryos injected with Activated Smo (0.63 pg/pl). AA29 is a marker for all non-skeletogenic cells; GCM is an early activator of NSM and necessary for pigment cell specification; Scl, is a marker activated prior to mesenchyme stage in NSM and necessary for blastocoelar cell specification. Both the Ptc MASO and Activated Smo had phenotypes at the pluteus stage but had no noticeable effect on expression of these three NSM markers at the mesenchyme blastula stage.

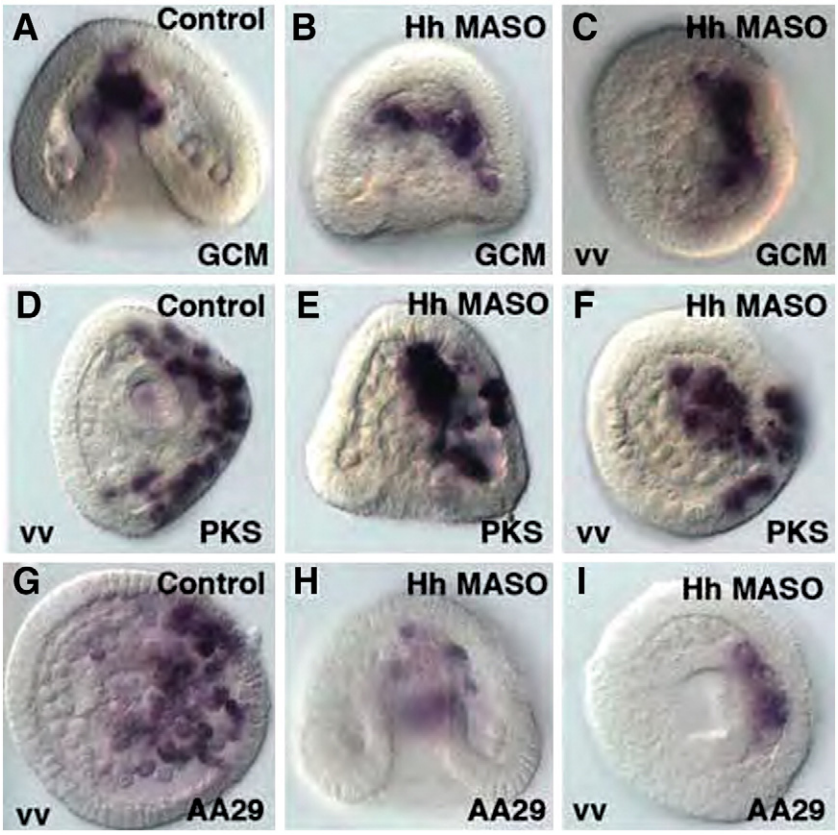

Fig. 5. Hedgehog knockdowns do not affect expression of endomesoderm GRN components at late gastrula stage. GCM normally is expressed in the aboral NSM and in pigment cells at late gastrula (A). Embryos injected with Hh MASO at concentrations that affect late patterning nevertheless express GCM normally (B, C). PKS is a differentiation gene in the pigment cell lineage and pigment cells invade ectoderm on the aboral side (D). Hh MASO knockdowns do not alter PKS expression nor the ectodermal invasion (E, F). AA29 stains a number of NSM cells at late gastrula (G), and that staining pattern is not significantly altered in Hh MASO knockdowns (H, I). vv = ventral view.

et al., 2003). In control embryos, the entire vegetal ring of NSM is visible with stronger staining on the pigment cell (aboral) side of the ring (Figs. 4A, D). Embryos injected with Ptc MASO or ActSmo express AA29 at the mesenchyme blastula stage with no difference seen between control and perturbed embryos (Figs. 4B, E and C, F). GCM is a transcription factor necessary for pigment cell specification (Calestani et al., 2003; Ransick et al., 2002) and is expressed in the aboral half of the NSM ring by the mesenchyme blastula stage (Figs. 4G, J). This marker was expressed in both Ptc MASO and ActSmo perturbed embryos in the same pattern as in controls (Figs. 4H, K and I, L). Finally, Scl, which is highly expressed in blastocoelar cells (Hibino et al., 2006b), again displayed a similar pattern of expression in control and perturbed embryos (compare Figs. 4N, Q and O, R with M, P). Thus perturbation of Hh pathway members does not appear to alter distribution of NSM cells when examined at the mesenchyme blastula stage. We then turned to later events in embryogenesis that appeared to be altered by the perturbations.

Fig. 5 shows markers and transcription factors in the known endomesoderm GRN at late gastrulation, after the Hh pathway becomes active (assuming that it becomes active shortly after Hh is first transcribed at late mesenchyme blastula stage). GCM continues to be expressed in the NSM at the tip of the archenteron and in pigment cells that have invaded the ectoderm (Fig. 5A), and that pattern is not altered in the Hh morpholino knockdowns (Figs. 5B, C). PKS is a differentiation gene in the pigment cell pathway that is downstream of GCM in the endomesoderm GRN. Its expression and pattern of expression in the aboral ectoderm are also very similar in the Hh knockdowns (Figs. 5E, F), relative to control embryos (Fig. 5D). Finally, AA29 is also expressed in an unaltered pattern in the Hh knockdowns relative to controls (Figs. 5H, I compared to G). There may be a decrease in message level for the experimentals relative to controls but was not consistently seen in trials.

Hh signaling randomizes left/right coelomic pouch asymmetry, but does not affect ectodermal left/right asymmetry

Coelomic pouches and the circumesophageal muscle are NSM derivatives that appear after gastrulation. Although the mechanisms by which these structures diversify from other NSM tissues are not known, Duboc et al. (2005) showed that Nodal is important for differentially patterning the right and left coelomic pouches. Downstream of Nodal, soxE normally is expressed in the left coelomic pouch (Figs. 6A, A′). We asked if altered Hh signaling interfered with the expression and/or patterning of soxE in the coelomic pouch. ActSmo was injected into eggs, and plutei were later examined for soxE expression by situ hybridization. Figs. 6A2, A2* show that soxE was expressed in ActSmo-injected larvae as in controls and the expression was limited to one side of the coelomic pouch at the early pluteus stage (Fig. 6). Strikingly, however, in ActSmo-injected plutei soxE expression was randomized so that it was on the left side in 57.7% of larvae (Figs. 6A2, A2*) and on the right side in 42.3% of larvae (Figs. 6A3, A3*) ($n = 45$), while control larvae soxE expression was localized to the left coelomic pouch in 100% of the plutei examined ($n = 56$). Thus, altered Hh signaling modified the late patterning of coelomic pouches, an NSM derivative.

The left–right asymmetric patterning of the coelomic pouch mesoderm is driven by the asymmetric distribution of Nodal in the ectoderm (Duboc et al., 2005). Thus, it was possible the Hh perturbation somehow altered Nodal signaling. Accordingly, ActSmo RNA-injected embryos were examined for Nodal expression by in situ

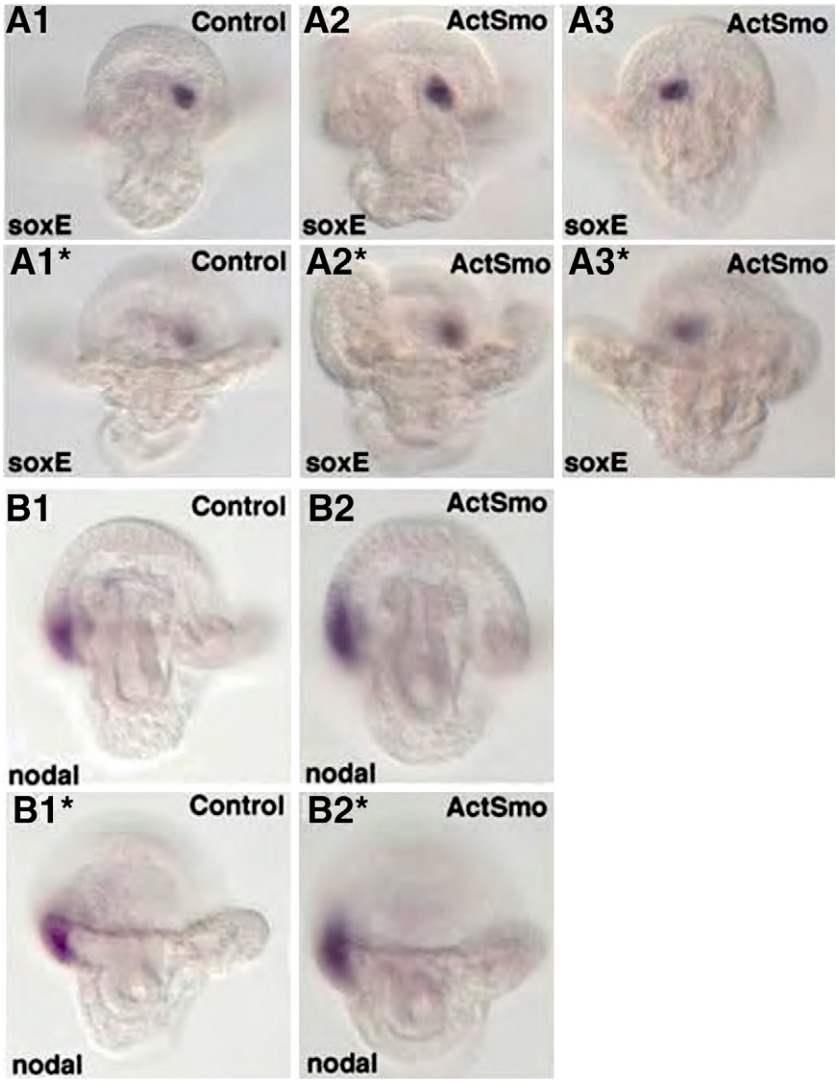

Fig. 6. Increased Hh signaling randomizes left–right asymmetry of the coelomic pouch expression of *soxE*, but not the ectodermal asymmetry of *Nodal* expression. RNA in situ hybridization with the normally left coelomic pouch marker, *soxE* (A), and the right-side ectodermal marker, *nodal* (B) were examined at the pluteus larval stage. Images of larvae in (A1–A3) are focused on the *soxE* positive cells and (B1, B2) are focused on the *nodal* expressing cells. (A1*–A3*) are the same larvae as in (A1–A3) and (B1 and B2) are the same larvae as in (B1* and B2*), but the focus is on the anal arms to provide orientation of the markers within the larvae. A1–A1* is a control larva hybridized with *soxE*. A2–A2* is a larva with normal left sided expression of *soxE*. A3–A3* is a larva with right-sided expression of *soxE*. B1–B1* is a control larva, while B2, B2* is a larva injected with ActSmo mRNA that have been and probed with *nodal*.

hybridization. Nodal in controls was expressed by ectoderm on the right side in 96.7% of the embryos (Figs. 6B1, B1*) ($n=31$), and embryos expressing ActSmo expressed Nodal correctly on the right side in 85.7% of all embryos examined (Figs. 6B2, B2*) ($n=28$). We conclude that while ectodermal Nodal expression was not randomized by increased Hh signaling, the gene regulatory networks in the right and left coelomic pouches were influenced by altered Hh signaling.

Increased Hh signaling mis-patterns muscle and alters muscle behavior

After Hh pathway perturbations larvae formed but did not grow. A closer look suggested that perturbed larvae thus treated could not feed normally. Under Nomarski optics the gut of Ptc MASO or ActSmo-injected larvae did not execute normal movements, suggesting that muscles were affected. This prompted us to ask whether the Hh-perturbed embryos were capable of swallowing. Control larvae or larvae injected with Ptc MASO or ActSmo were fed 10 μm polystyrene beads for 30 min. The control larvae swallowed continuously and their midguts were filled with polystyrene beads after 30 min (Figs. 7A, A′). In contrast, larvae with increased Hh signaling swallowed few beads, if any, during the same period of time (Figs. 7B, B′ and C, C′), or even after an hour (data not shown). The perturbed larvae had mouths and the beads were brought into the mouth area by movement of the ciliary band feeding mechanism (Fig. 7B), but the beads were not swallowed. Perturbed larvae moved the pharynx and gut, showing the presence of some muscle contraction, but the contractions failed to generate a coordinated peristaltic movement as seen in control embryos.

To detail muscle pattern changes, an anti-myosin antibody was used to stain the circumesophageal muscle of the embryo (Fig. 8). Muscle fibers were disarrayed in Ptc MASO-injected embryos (Fig. 8C), and ActSmo-injected embryos (Fig. 8D) relative to controls (Fig. 8B), as first seen when Hh was knocked down in earlier experiments (see Fig. 3D). These alterations in muscle patterning included a decrease in muscle area and a decrease in the number of fibers, although the fibers remaining appeared thicker than controls. Measurements of the muscle dimensions revealed that the Ptc MASO-injected embryos had a 32% reduction in muscle area on the ventral side as compared to control embryos. The dorsal side and diameter of the musculature

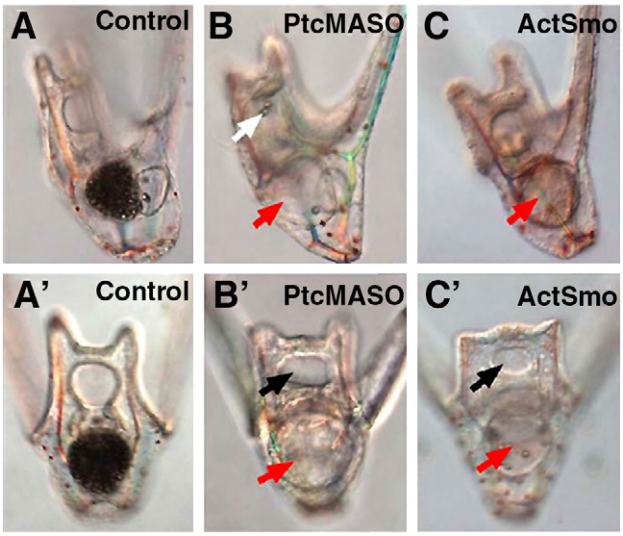

Fig. 7. Test of swallowing and peristalsis. The ability to swallow was examined by feeding latex beads for 1 h to 2-day-old larvae. Control larvae have midguts filled with swallowed beads (A1 and A1′). Ptc MASO-injected larvae (0.75 mM) (A2 and A2′), and ActSmo injected larvae (0.63 pg/pl) (A3 and A3′) fail to swallow the beads. Red arrows show midguts with very few beads in larvae with increased Hh signaling. Black arrows show that mouths do form in those larvae. White arrow indicates that beads enter the mouth of those embryos but those entering beads fail to be swallowed.

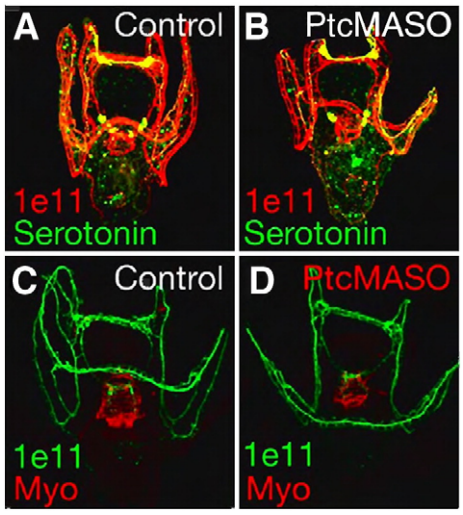

Fig. 9. Patterning of serotonergic and non-serotonergic neurons throughout the larvae shown by confocal projections of fluorescent nerve markers. Anti-serotonin (green) shows a normal pattern of serotonergic neurons in both control (A) and Ptc MASO-injected embryos (B). Anti-Synaptotagmin B shows all neurons in red in control embryos (A) and in Ptc MASO-injected embryos (B) and in green in (C, D). Myosin antibody staining in red (C, D) shows a normal pattern of circumesophageal muscle in the pharynx (C) and an abnormal pattern in the Ptc MASO-injected embryos (D).

was less affected. Therefore, muscle fibers were mis-patterned and reduced in area when Hh signaling was perturbed.

In the sea urchin, neurons project to the muscle and the underlying endoderm (Nakajima et al., 2004), to regulate among other properties, the peristaltic movement of swallowing. To ask if neural elements were included in the Hh pathway disruptions we first examined the organization of the nerves innervating the gut muscle. The antibody marker 1e11 stains the general nerve marker Synaptotagmin (Burke et al., 2006), and an antibody to Serotonin stains serotonergic neurons in the sea urchin (Yaguchi et al., 2006). Both serotonergic and non-serotonergic neurons were present and properly localized in Ptc MASO-injected larvae when compared to control larvae (Figs. 9A versus B). In addition, 1e11 staining revealed nerves throughout the oral hood and arms and these were well organized and very similar to controls (Figs. 9C and D). The nerves around the gut were also present and located directly beneath the muscle fibers so the organization of the circumesophageal nerves in perturbed embryos appeared identical to those in control larvae. Thus, the pattern of the neural circuitry did not appear to be affected by Hh pathway perturbations.

Even though the neural circuitry appeared normal anatomically, it was possible that neural function was altered by Hh perturbations. This was addressed in recombination studies. The animal half of the embryo gives rise to the ectoderm of the embryo from which the neurons are derived (Yaguchi et al., 2006). The vegetal half gives rise to mesoderm, and endoderm (Davidson et al., 1998; Logan and McClay, 1997), from which the muscles originate. Reciprocal transplantation experiments recombined animal and vegetal halves from control-injected and Ptc MASO-injected embryos (Fig. 10). Abnormal muscle patterning and behavior occurred only when the vegetal half of the recombinant was perturbed (Figs. 10C, E), as there was no effect when Ptc MASO was present in the animal half (Figs. 10B, D). Therefore, Hh signaling is required in the vegetal half of the embryo (from which the muscles are derived) for proper peristaltic movements and those movements were unaffected when the perturbation was restricted to the animal half (where nerves are produced). This experiment also revealed another aspect of pattern disruption in the embryo. Earlier it was noted that skeletal patterning was disrupted by Hh pathway perturbations (Figs. 2 and 3). Previous work had shown that patterning information for skeletogenesis is provided by the ectoderm (Armstrong et al., 1993; Armstrong and McClay, 1994; Hardin et al., 1992). The chimera experiments revealed skeletal defects in embryos only when the vegetal half of the embryo contained perturbed Hh pathway components. When the perturbation was in the animal half of the recombinants there were no observable skeletogenic defects. Thus the Hh pathway appears to operate only on mesodermal structures, and not by way of the ectoderm, which provides patterning input for skeletogenesis, coelomic pouch patterning, and neurogenesis.

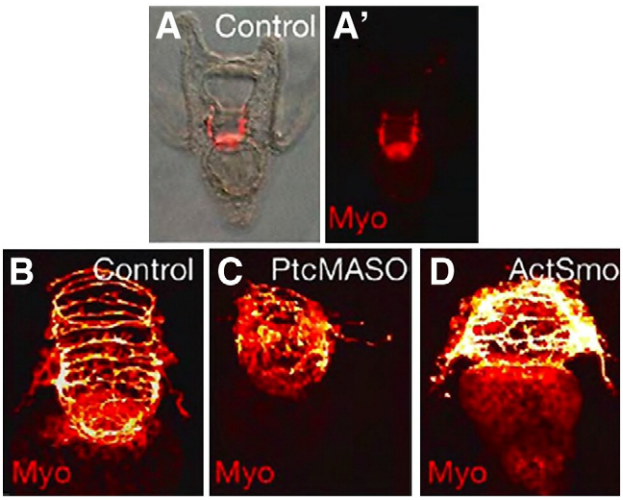

Fig. 8. Myosin antibody staining shows circumesophageal muscle organization in 48 h control embryos (A, A′, B). In 48 h embryos injected with Ptc MASO (0.75 mM) (C), and in 48 h embryos expressing ActSmo (0.63 pg/pl) (D), the circumesophageal muscle is patterned abnormally compared to the control. Images are captured by DIC (A), fluorescence microscopy (A′), and by confocal microscopy (B–D).

Discussion

In the sea urchin embryo Hh signaling functions as a paracrine signal with Hh expressed in the endoderm and its receptors Ptc and Smo, expressed largely, if not exclusively, in the mesoderm, both in the

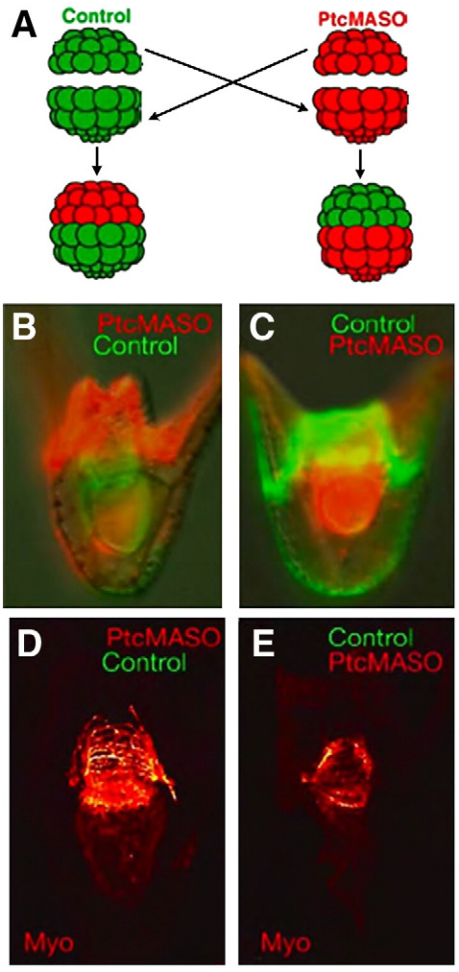

Fig. 10. Reciprocal transplantation of animal and vegetal halves from control and Ptc MASO-injected embryos (0.75 mM). (A) shows a diagram of the experiment. A control animal half (green) is placed on a red Ptc MASO-injected vegetal half, and reciprocally, a red Ptc-MASO-injected animal half is placed on a green control vegetal half. 48 h embryos in which the Ptc MASO was in the animal half (B, D) and reciprocally, in which the Ptc MASO was in the vegetal half (C, E). The fluorescent lineage tracers are shown in (B, C), and (D, E) show the circumesophageal muscle of the embryo immediately above them as seen by confocal microscopy. When the Ptc MASO is in the vegetal half the muscle patterning is abnormal (E), while if the Ptc MASO is in the animal half the muscle pattern is normal (D).

NSM and PMCs. Perturbation of Hh signaling, up or down, results in altered numbers and/or abnormal patterning of mesodermally derived tissues, both skeletogenic and non-skeletogenic. The number of pigment cells was increased with activation of the pathway and decreased with inhibition of the pathway suggesting a role for the pathway in subdividing the NSM territory. Increased Hh signaling randomized the left–right asymmetry of the coelomic pouches, disorganized circumesophageal muscles leading to an inability of the larva to swallow, and disrupted normal skeletal patterning. In each case early specification of the affected cells seemed to be normal but the PMC and NSM structures were mis-patterned after the Hh pathway was activated at the beginning of gastrulation. Thus Hh signaling is involved, not in early specification, but in later patterning of tissues derived from mesoderm in the sea urchin embryo.

Hh signaling, a paracrine versus autocrine signal in sea urchin?

Hh is known to act as not only a paracrine signal, but as an autocrine signal as well. Examples of this are observed in both heart development and tooth development in mouse (Goddeeris et al., 2007; Wu et al., 2003). In our experiments Ptc and Smo were not detected in endoderm with the possible exception of a low level in the late hindgut near the ectoderm–endoderm boundary. Hh, by contrast, was observed only in the endoderm. When the Hh pathway was perturbed we often observed a delayed invagination of the archenteron (e.g. altered Ptc expression in Fig. 2). Since the NSM leads the process of invagination, and since perturbations of that morphogenetic process are mediated initially through the NSM (Beane et al., 2006; Croce et al., 2006), it is most likely that the Hh perturbations affecting gastrulation acted exclusively through the NSM. Mesodermal feedback to the endoderm following the response to Hh signal is also a possibility that cannot be ruled out. In patterning of the chick intestinal tract, for example, bidirectional signals emanate from the endoderm and mesoderm to pattern the reciprocal tissue (Kedinger et al., 1998; Li et al., 2007). Absence of one affects the other. In the mouse intestine Shh is expressed in the endodermal epithelium and Ptc1 is expressed in the neighboring mesoderm; alterations in Hh signaling produce mesodermal expansion and mis-patterning which then secondarily affects endodermal epithelial formation (Madison et al., 2005).

It may seem odd that the entire endoderm expresses Hh since its signal seems to function only in the adjacent mesodermal territories, however this is not unprecedented. In vertebrates Shh is produced throughout the gut yet there is regional reception of the Shh signal by mesoderm cells, presumably by mesoderm cells that are differentially receptive, relative to other mesoderm cells (Roberts et al., 1998). Also, in *Drosophila* wings Hh is expressed in the entire posterior half of the wing imaginal disc, yet the Hh signaling occurs only at the anterior–posterior boundary where Ptc is expressed most highly (Tabata and Kornberg, 1994). In the sea urchin, Hh is expressed along the entire gut from the beginning of gastrulation until the pluteus larval stage. Hh is expressed in the foregut directly adjacent to the budding coelomic pouches and circumesophageal muscle, and in the hindgut, adjacent to the PMCs, which also appear to rely on Hh signaling for components of their patterning. Mesodermal expression of Ptc and Smo persists until at pluteus stage when their expression becomes restricted to NSM cells surrounding the esophagus, areas where the coelomic pouches and the circumesophageal muscles are patterned. Thus, Hh signaling appears to continue from endoderm to mesoderm over a long span of developmental time. Currently the temporal details of that signaling are unknown, other than they occur later than the timeframe covered by the current endomesoderm GRN (Davidson et al., 2002).

Hh signaling and its relationship to Nodal signaling and left–right asymmetry

In indirect-developing species of sea urchins the left coelomic pouch becomes the rudiment of the adult sea urchin at metamorphosis. Although the detailed mechanism for establishing this asymmetrical assignment is not understood, recent studies have greatly advanced our knowledge by identifying Nodal as an essential signal for the process (Hibino et al., 2006a; (Duboc et al., 2005). That asymmetrical assignment is quite robust as demonstrated by experiments with halved *L. variegatus* embryos. Each half embryo was able to regulate and replace correctly the missing sides up until the mesenchyme blastula stage (McCain and McClay, 1994). In two other indirect-developing species of sea urchin, a series of surgical excisions of embryo portions showed that the right-side ectoderm and/or coelomic pouch mesoderm conveys a signal to the left side to direct rudiment development there (Aihara and Amemiya, 2001). Nodal was identified as a right-side signal; its expression on the right side of the ectoderm is essential for defining the left–right asymmetry of the coelomic pouch and restricting rudiment formation to the left side (Duboc et al., 2005). Since perturbation of Hh signaling randomized placement of left–right markers in the coelomic pouches and did not

affect the normal right-side expression of Nodal in ectoderm, the Hh pathway must disturb aspects downstream of the reception of the Nodal signal in the coelomic pouches.

Hh plays multiple roles in supplying patterning information for mesoderm development

It is not unusual for Hh to have multiple roles governing patterning in a single embryo. In vertebrates Shh patterns limb buds, the floor plate of the neural tube, and subdivision of endodermal organs, just to mention a few roles. Thus it should come as no surprise that Hh has multiple roles in the sea urchin. Ptc and Smo are in PMC ventrolateral clusters where skeletogenesis begins. Perturbations of Ptc, Smo, or Hh cause skeletal mis-patterning. Other reports previously suggested endodermal involvement in skeletal patterning without knowing the pathway (Benink et al., 1997; Croce et al., 2006). This report demonstrates one such endodermal signal that signals to PMCs, but whether it is the only endoderm-to-PMC signal is unknown. Other recent reports have shown that VEGF and FGF signals from the ectoderm are important for skeletal patterning (Duloquin et al., 2007; Rottinger et al., 2008). The addition of Hh signaling to the patterning of the larval skeleton thus adds to the complexity of the signals involved. The separate role for each of these signals in establishing the easel-shaped skeleton remains to be determined.

Hh pathway perturbations affected the number of pigment and blastocoelar cells. The expansion of pigment and blastocoelar cells with increased Hh pathway signaling, though statistically well supported, is modest and could come at the expense of endoderm and/or the remaining two NSM subtypes, coelomic pouch and muscle. We were unable to find significant changes in endoderm cell numbers though we cannot rule out the loss of a few cells per embryo. From previous experiments we know that the NSM is capable of replacing endoderm, and that endoderm is capable of regulating to replace NSM (McClay and Logan, 1996). It is possible that the Hh pathway is involved in establishing or maintaining those later identities. Augmented Hh signaling has been shown to enhance proliferation and survival in a variety of tumors and tissues including the mesoderm (Ahlgren et al., 2002; Cayuso et al., 2006; Feng et al., 2006; Hallahan et al., 2004; Hutchin et al., 2005; Kruger et al., 2001; Morton et al., 2007; Yu et al., 2002; Zhang et al., 2001), so the modified numbers of cells resulting from Hh perturbations is not unprecedented.

Expression of Hh is dependent upon FoxA and Brachyury; loss of FoxA through MASO knockdown in *S. purpuratus* and *L. variegatus* results in a loss of Hh mRNA (Oliveri et al., 2006), and later, abnormal patterning. Likewise, increased Hh signaling results in alterations in mesodermal patterning. Together these results suggest a model in which the endodermally derived FoxA repressor inhibits a negative regulator of Hh expression, thus leading to transcription of Hh. The Hh signal is secreted and acts in a paracrine fashion to pattern structures derived in the mesoderm. As yet the endomesoderm gene regulatory network is well understood only until the beginning of gastrulation. As such, at least there is information that connects initial expression of Hh to that network model. To understand later events of morphogenesis, differentiation of cell types and patterning, it is necessary to extend the endomesoderm GRN to later stages, and the Hh pathway will be an important component of that extension.

Acknowledgments

We thank Dr. Jenifer Croce, Dr. Cynthia Bradham, Dr. Wendy Beane and Dr. Shu-Yu Wu for helpful insights and critical comments. Dr. Sam Johnson provided imaging advice. Dr. Gary Wessel produced the myosin antibody, a small amount of which was provided by Dr. Lynne Angerer. Funding for this research was provided by NIH grants HD14483, GM61464 and PO50 GM081883 to D.R.M. and a Fellowship from the U.S. Army Medical Research and Materiel Command under W81XWH-04-1-0324 to K.D.W.

References

Ahlgren, S.C., Thakur, V., Bronner-Fraser, M., 2002. Sonic hedgehog rescues cranial neural crest from cell death induced by ethanol exposure. Proc. Natl. Acad. Sci. U. S. A. 99, 10476–10481.

Aihara, M., Amemiya, S., 2001. Left–right positioning of the adult rudiment in sea urchin larvae is directed by the right side. Development 128, 4935–4948.

Armstrong, N., McClay, D.R., 1994. Skeletal pattern is specified autonomously by the primary mesenchyme cells in sea urchin embryos. Dev. Biol. 162, 329–338.

Armstrong, N., Hardin, J., McClay, D.R., 1993. Cell–cell interactions regulate skeleton formation in the sea urchin embryo. Development 119, 833–840.

Aspock, G., Kagoshima, H., Niklaus, G., Burglin, T.R., 1999. *Caenorhabditis elegans* has scores of hedgehog-related genes: sequence and expression analysis. Genome Res. 9, 909–923.

Beach, R.L., Seo, P., Venuti, J.M., 1999. Expression of the sea urchin MyoD homologue, SUM1, is not restricted to the myogenic lineage during embryogenesis. Mech. Dev. 86, 209–212.

Beane, W.S., Gross, J.M., McClay, D.R., 2006. RhoA regulates initiation of invagination, but not convergent extension, during sea urchin gastrulation. Dev. Biol. 292, 213–225.

Benink, H., Wray, G., Hardin, J., 1997. Archenteron precursor cells can organize secondary axial structures in the sea urchin embryo. Development 124, 3461–3470.

Burke, R.D., Alvarez, C.M., 1988. Development of the esophageal muscles in embryos of the sea urchin *Strongylocentrotus purpuratus*. Cell Tissue Res. 252, 411–417.

Burke, R.D., Osborne, L., Wang, D., Murabe, N., Yaguchi, S., Nakajima, Y., 2006. Neuron-specific expression of a synaptotagmin gene in the sea urchin *Strongylocentrotus purpuratus*. J. Comp. Neurol. 496, 244–251.

Calestani, C., Rast, J.P., Davidson, E.H., 2003. Isolation of pigment cell specific genes in the sea urchin embryo by differential macroarray screening. Development 130, 4587–4596.

Cayuso, J., Ulloa, F., Cox, B., Briscoe, J., Marti, E., 2006. The Sonic hedgehog pathway independently controls the patterning, proliferation and survival of neuroepithelial cells by regulating Gli activity. Development 133, 517–528.

Chang, D.T., Lopez, A., von Kessler, D.P., Chiang, C., Simandl, B.K., Zhao, R., Seldin, M.F., Fallon, J.F., Beachy, P.A., 1994. Products, genetic linkage and limb patterning activity of a murine hedgehog gene. Development 120, 3339–3353.

Croce, J., Lhomond, G., Gache, C., 2003. Coquillette, a sea urchin T-box gene of the Tbx2 subfamily, is expressed asymmetrically along the oral–aboral axis of the embryo and is involved in skeletogenesis. Mech. Dev. 120, 561–572.

Croce, J., Duloquin, L., Lhomond, G., McClay, D.R., Gache, C., 2006. Frizzled5/8 is required in secondary mesenchyme cells to initiate archenteron invagination during sea urchin development. Development 133, 547–557.

Davidson, E.H., Cameron, R.A., Ransick, A., 1998. Specification of cell fate in the sea urchin embryo: summary and some proposed mechanisms. Development 125, 3269–3290.

Davidson, E.H., Rast, J.P., Oliveri, P., Ransick, A., Calestani, C., Yuh, C.H., Minokawa, T., Amore, G., Hinman, V., Arenas-Mena, C., Otim, O., Brown, C.T., Livi, C.B., Lee, P.Y., Revilla, R., Schilstra, M.J., Clarke, P.J., Rust, A.G., Pan, Z., Arnone, M.I., Rowen, L., Cameron, R.A., McClay, D.R., Hood, L., Bolouri, H., 2002. A provisional regulatory gene network for specification of endomesoderm in the sea urchin embryo. Dev. Biol. 246, 162–190.

Duboc, V., Rottinger, E., Lapraz, F., Besnardeau, L., Lepage, T., 2005. Left–right asymmetry in the sea urchin embryo is regulated by nodal signaling on the right side. Dev. Cell. 9, 147–158.

Duloquin, L., Lhomond, G., Gache, C., 2007. Localized VEGF signaling from ectoderm to mesenchyme cells controls morphogenesis of the sea urchin embryo skeleton. Development 134, 2293–2302.

Echelard, Y., Epstein, D.J., St-Jacques, B., Shen, L., Mohler, J., McMahon, J.A., McMahon, A.P., 1993. Sonic hedgehog, a member of a family of putative signaling molecules, is implicated in the regulation of CNS polarity. Cell 75, 1417–1430.

Egana, A.L., Ernst, S.G., 2004. Sphedgehog is expressed by pigment cell precursors during early gastrulation in *Strongylocentrotus purpuratus*. Dev. Dyn. 231, 370–378.

Feng, X., Adiarte, E.G., Devoto, S.H., 2006. Hedgehog acts directly on the zebrafish dermomyotome to promote myogenic differentiation. Dev. Biol. 300, 736–746.

Goddeeris, M.M., Schwartz, R., Klingensmith, J., Meyers, E.N., 2007. Independent requirements for Hedgehog signaling by both the anterior heart field and neural crest cells for outflow tract development. Development 134, 1593–1604.

Gustafson, T., Wolpert, L., 1963. Studies on the cellular basis of morphogenesis in the sea urchin embryo. Formation of the coelom, the mouth, and the primary pore-canal. Exp. Cell Res. 29, 561–582.

Hallahan, A.R., Pritchard, J.I., Hansen, S., Benson, M., Stoeck, J., Hatton, B.A., Russell, T.L., Ellenbogen, R.G., Bernstein, I.D., Beachy, P.A., Olson, J.M., 2004. The SmoA1 mouse model reveals that notch signaling is critical for the growth and survival of sonic hedgehog-induced medulloblastomas. Cancer Res. 64, 7794–7800.

Hardin, J., Coffman, J.A., Black, S.D., McClay, D.R., 1992. Commitment along the dorsoventral axis of the sea urchin embryo is altered in response to NiCl2. Development 116, 671–685.

Hibino, T., Ishii, Y., Levin, M., Nishino, A., 2006a. Ion flow regulates left–right asymmetry in sea urchin development. Dev. Genes Evol. 216, 265–276.

Hibino, T., Loza-Coll, M., Messier, C., Majeske, A.J., Cohen, A.H., Terwilliger, D.P., Buckley, K.M., Brockton, V., Nair, S.V., Berney, K., Fugmann, S.D., Anderson, M.K., Pancer, Z., Cameron, R.A., Smith, L.C., Rast, J.P., 2006b. The immune gene repertoire encoded in the purple sea urchin genome. Dev. Biol. 300, 349–365.

Huangfu, D., Anderson, K.V., 2006. Signaling from Smo to Ci/Gli: conservation and divergence of Hedgehog pathways from *Drosophila* to vertebrates. Development 133, 3–14.
Hutchin, M.E., Kariapper, M.S., Grachtchouk, M., Wang, A., Wei, L., Cummings, D., Liu, J., Michael, L.E., Glick, A., Dlugosz, A.A., 2005. Sustained Hedgehog signaling is required for basal cell carcinoma proliferation and survival: conditional skin tumorigenesis recapitulates the hair growth cycle. Genes Dev. 19, 214–223.
Ingham, P.W., McMahon, A.P., 2001. Hedgehog signaling in animal development: paradigms and principles. Genes Dev. 15, 3059–3087.
Kang, D., Huang, F., Li, D., Shankland, M., Gaffield, W., Weisblat, D.A., 2003. A hedgehog homolog regulates gut formation in leech (Helobdella). Development 130, 1645–1657.
Kedinger, M., Duluc, I., Fritsch, C., Lorentz, O., Plateroti, M., Freund, J.N., 1998. Intestinal epithelial–mesenchymal cell interactions. Ann. N.Y. Acad. Sci. 859, 1–17.
Krauss, S., Concordet, J.P., Ingham, P.W., 1993. A functionally conserved homolog of the *Drosophila* segment polarity gene hh is expressed in tissues with polarizing activity in zebrafish embryos. Cell 75, 1431–1444.
Kruger, M., Mennerich, D., Fees, S., Schafer, R., Mundlos, S., Braun, T., 2001. Sonic hedgehog is a survival factor for hypaxial muscles during mouse development. Development 128, 743–752.
Kuwabara, P.E., Lee, M.H., Schedl, T., Jefferis, G.S., 2000. A *C. elegans* patched gene, ptc-1, functions in germ-line cytokinesis. Genes Dev. 14, 1933–1944.
Lepage, T., Gache, C., 1990. Early expression of a collagenase-like hatching enzyme gene in the sea urchin embryo. EMBO J. 9, 3003–3012.
Li, X., Madison, B.B., Zacharias, W., Kolterud, A., States, D., Gumucio, D.L., 2007. Deconvoluting the intestine: molecular evidence for a major role of the mesenchyme in the modulation of signaling cross talk. Physiol. Genomics 29, 290–301.
Logan, C.Y., McClay, D.R., 1997. The allocation of early blastomeres to the ectoderm and endoderm is variable in the sea urchin embryo. Development 124, 2213–2223.
Lum, L., Beachy, P.A., 2004. The Hedgehog response network: sensors, switches, and routers. Science 304, 1755–1759.
Madison, B.B., Braunstein, K., Kuizon, E., Portman, K., Qiao, X.T., Gumucio, D.L., 2005. Epithelial hedgehog signals pattern the intestinal crypt-villus axis. Development 132, 279–289.
Matus, D.Q., Magie, C., Pang, K., Martindale, M.Q., Thomsen, G.H., 2007. The Hedgehog gene family of the cnidarian, *Nematostella vectensis*, and implications for understanding metazoan Hedgehog pathway evolution. Dev. Biol. 313, 501–518.
McCain, E.R., McClay, D.R., 1994. Establishment of bilateral asymmetry in the sea urchin *Lytechinus variegatus*. Development 120, 395–404.
McClay, D.R., Logan, C.Y., 1996. Regulative capacity of the archenteron during gastrulation in the sea urchin. Development 122, 607–616.
McClay, D.R., Cannon, G.W., Wessel, G.M., Fink, R.D., Marchase, R.B., 1983. Patterns of antigenic expression in early sea urchin development. In: Jeffrey, W.R., Raff, R.A. (Eds.), Time, Space, and Pattern in Embryonic Development, 69. Alan R. Liss, Inc., New York., pp. 157–169.
Morton, J.P., Mongeau, M.E., Klimstra, D.S., Morris, J.P., Lee, Y.C., Kawaguchi, Y., Wright, C.V., Hebrok, M., Lewis, B.C., 2007. Sonic hedgehog acts at multiple stages during pancreatic tumorigenesis. Proc. Natl. Acad. Sci. U. S. A. 104, 5103–5108.
Nakajima, Y., Kaneko, H., Murray, G., Burke, R.D., 2004. Divergent patterns of neural development in larval echinoids and asteroids. Evol. Dev. 6, 95–104.
Oliveri, P., Walton, K.D., Davidson, E.H., McClay, D.R., 2006. Repression of mesodermal fate by foxa, a key endoderm regulator of the sea urchin embryo. Development 133, 4173–4181.
Peterson, R.E., McClay, D.R., 2003. Primary mesenchyme cell patterning during the early stages following ingression. Dev. Biol. 254, 68–78.
Ransick, A., Rast, J.P., Minokawa, T., Calestani, C., Davidson, E.H., 2002. New early zygotic regulators expressed in endomesoderm of sea urchin embryos discovered by differential array hybridization. Dev. Biol. 246, 132–147.
Rast, J.P., Smith, L.C., Loza-Coll, M., Hibino, T., Litman, G.W., 2006. Genomic insights into the immune system of the sea urchin. Science 314, 952–956.
Riddle, R.D., Johnson, R.L., Laufer, E., Tabin, C., 1993. Sonic hedgehog mediates the polarizing activity of the ZPA. Cell 75, 1401–1416.
Roberts, D.J., Smith, D.M., Goff, D.J., Tabin, C.J., 1998. Epithelial–mesenchymal signaling during the regionalization of the chick gut. Development 125, 2791–2801.
Roelink, H., Augsburger, A., Heemskerk, J., Korzh, V., Norlin, S., Altaba, A.R.I., Tanabe, Y., Placzek, M., Edlund, T., Jessell, T.M., Dodd, J., 1994. Floor plate and motor neuron induction by Vhh-1, a vertebrate homolog of hedgehog expressed by the notochord. Cell 76, 761–775.
Rottinger, E., Saudemont, A., Duboc, V., Besnardeau, L., McClay, D., Lepage, T., 2008. FGF signals guide migration of mesenchymal cells, control skeletal morphogenesis [corrected] and regulate gastrulation during sea urchin development. Development 135, 353–365.
Shimeld, S.M., 1999. The evolution of the hedgehog gene family in chordates: insights from amphioxus hedgehog. Dev. Genes Evol. 209, 40–47.
Sweet, H.C., Hodor, P.G., Ettensohn, C.A., 1999. The role of micromere signaling in notch activation and mesoderm specification during sea urchin embryogenesis. Development 126, 5255–5265.
Sweet, H.C., Gehring, M., Ettensohn, C.A., 2002. LvDelta is a mesoderm-inducing signal in the sea urchin embryo and can endow blastomeres with organizer-like properties. Development 129, 1945–1955.
Tabata, T., Kornberg, T.B., 1994. Hedgehog is a signaling protein with a key role in patterning *Drosophila* imaginal discs. Cell 76, 89–102.
Taipale, J., Chen, J.K., Cooper, M.K., Wang, B., Mann, R.K., Milenkovic, L., Scott, M.P., Beachy, P.A., 2000. Effects of oncogenic mutations in Smoothened and Patched can be reversed by cyclopamine. Nature 406, 1005–1009.
Venuti, J.M., Goldberg, L., Chakraborty, T., Olson, E.N., Klein, W.H., 1991. A myogenic factor from sea urchin embryos capable of programming muscle differentiation in mammalian cells. Proc. Natl. Acad. Sci. U. S. A. 88, 6219–6223.
Venuti, J.M., Gan, L., Kozlowski, M.T., Klein, W.H., 1993. Developmental potential of muscle cell progenitors and the myogenic factor SUM-1 in the sea urchin embryo. Mech. Dev. 41, 3–14.
Walton, K.D., Croce, J.C., Glenn, T.D., Wu, S.Y., McClay, D.R., 2006. Genomics and expression profiles of the Hedgehog and Notch signaling pathways in sea urchin development. Dev. Biol. 300, 153–164.
Wessel, G.M., Zhang, W., Klein, W.H., 1990. Myosin heavy chain accumulates in dissimilar cell types of the macromere lineage in the sea urchin embryo. Dev. Biol. 140, 447–454.
Wu, C., Shimo, T., Liu, M., Pacifici, M., Koyama, E., 2003. Sonic hedgehog functions as a mitogen during bell stage of odontogenesis. Connect Tissue Res. 44 (Suppl. 1), 92–96.
Xie, J., Murone, M., Luoh, S.M., Ryan, A., Gu, Q., Zhang, C., Bonifas, J.M., Lam, C.W., Hynes, M., Goddard, A., Rosenthal, A., Epstein Jr., E.H., de Sauvage, F.J., 1998. Activating Smoothened mutations in sporadic basal-cell carcinoma. Nature 391, 90–92.
Yaguchi, S., Yaguchi, J., Burke, R.D., 2006. Specification of ectoderm restricts the size of the animal plate and patterns neurogenesis in sea urchin embryos. Development 133, 2337–2346.
Yu, J., Carroll, T.J., McMahon, A.P., 2002. Sonic hedgehog regulates proliferation and differentiation of mesenchymal cells in the mouse metanephric kidney. Development 129, 5301–5312.
Zhang, X.M., Ramalho-Santos, M., McMahon, A.P., 2001. Smoothened mutants reveal redundant roles for Shh and Ihh signaling including regulation of L/R symmetry by the mouse node. Cell 106, 781–792.